

Imaging biotin trafficking *in vivo* with positron emission tomography

Salvatore Bongarzone¹, Teresa Sementa¹, Joel Dunn¹, Jayanta Bordoloi¹,
Kavitha Sunassee¹, Philip J. Blower¹ and Antony Gee¹

¹School of Biomedical Engineering & Imaging Sciences, King's College London, King's Health Partners, St Thomas' Hospital, London, SE1 7EH, United Kingdom.

SUPPORTING INFORMATION

Table of Contents

<i>Radiochemistry</i>	S2
<i>Preparation of the synthesis module</i>	S2
<i>In vitro [¹¹C]biotin-streptavidin binding</i>	S2
<i>[¹¹C]biotin-streptavidin binding assay</i>	S2
<i>Biodistribution and metabolite studies in mice</i>	S3
<i>Uptake and Excretion Clearances of [¹¹C]biotin</i>	S3
<i>Statistical analysis for Figure S9 and Table S3</i>	S3
<i>Figure S1: Schematic diagram of the automated synthesis of [¹¹C]biotin</i>	S4
<i>Figure S2 Radio-HPLC radiochromatogram of formulated [¹¹C]biotin on analytical HPLC</i>	S4
<i>Figure S3: Streptavidin–microspheres uptake of [¹¹C]biotin</i>	S5
<i>Figure S4. Schematic illustration of the PET/CT image acquisition of intravenous (IV) and orogastric gavage (OG) administration of formulation A and [¹¹C]biotin</i>	S5
<i>Figure S5: Time Activity curves of male and female mice receiving [¹¹C]biotin IV</i>	S6
<i>Figure S6 Correlation of blood radioactivity concentration from in vivo PET images versus ex vivo biodistribution</i>	S6
<i>Figure S7 Logan equation and Logan plots of kidney, liver, BAT and brain of groups A1-A3</i>	S7
<i>Figure S8 Patlak equation and Patlak plots of BAT and brain of groups A1-A3</i>	S8
<i>Figure S9: Biodistribution of radio activity after injection of [¹¹C]biotin in mice</i>	S9
<i>Figure S10: Time Activity curves of female mice receiving [¹¹C]biotin OG</i>	S9
<i>Table S1: Details of [¹¹C]biotin synthesis</i>	S10
<i>Table S2: Details of [¹¹C]biotin formulation administered to animal groups</i>	S10
<i>Table S3: Tissue/Blood Ratio for groups A1-A3</i>	S11
<i>References</i>	S11

Radiochemistry

Biotin, 1,8-Diazabicyclo[5.4.0]undec-7-ene (DBU), tributylphosphine (PBU₃), di-tert-butyl azodicarboxylate (DBAD), dry acetonitrile (MeCN), phosphate buffered saline tablets were obtained commercially from Sigma-Aldrich. (2S,3S,4R)-Cis-5-(3,4-Diaminotetrahydro-2-thienyl)valeric acid (diamino biotin) was obtained commercially from Insight Biotechnology.

Preparation of the synthesis module

The E&Z E & Z Eurotope GmbH (Berlin, Germany) “modular-lab” system was configured according to a [¹¹C]biotin synthesis sequence program (**Figure S1**). In this configuration, two Peltier reactor modules (PRM), which allows temperature control from -40°C to +150°C, was used. These reactors are equipped temperature and radioactivity sensors and a reactor camera. The reactions were carried out in an oven-dried vials (KX Microwave Vials, 2–5 mL) and crimp caps (Fisherbrand, centre hole with 3.0 mm PTFE seal aluminium silver 20 mm, part # 10132712). All the lines used to permit the flow of gases were PTFE tubing (length: 10–20 cm, outside diameter: 0.79 x 0.4 in., inside diameter: 1/32 x 0.16 in.). A P₂O₅ trap and one-way valve (BRAUN, normally closed backcheck valve, part #415062) were placed before Vial A. An ascarite trap consisting of a cartridge (Biosys Solutions Ltd, Fritted Empty MiniSpeed Cartridges, part # 2447) filled with ascarite (Sigma-Aldrich, 1310-73-2) and a Tedlar Gas Sampling Bags were placed after vial B to trap unreacted carbon-11 carbon dioxide ([¹¹C]CO₂). Transfers were controlled by the automatic switching of the in-line three-way valves on the modules. All processes are remotely controlled by a computer employing the dedicated modular-lab software interface from E&Z. At the end of radiosynthesis (after the complete decay of radioactivity), the system was cleaned by filling the reagent vials with sterile water, then acetonitrile, and lastly by a stream of helium. Cleaned and oven-dried vials and new tubing were used every time before starting a new [¹¹C]biotin batch production. Parts after preparative HPLC (i.e. valves, preparative sample loop, product outlet tubing, PTFE tubing) were replaced or cleaned using water and acetonitrile.

In vitro [¹¹C]biotin-streptavidin binding

To a 100 µL suspension of streptavidin magnetic particles was added 400 µL of a solution containing 150 mM of NaCl and 10 mM PBS (pH 7.4) in test tubes (1.5 mL). The streptavidin magnetic particles and supernatant were separated by SureBeads Magnetic Rack (Bio-Rad Laboratories, 1614916). The streptavidin magnetic particles were washed three times with 500 µL of buffer. After the wash the streptavidin magnetic particles were incubated for 5 minutes at 25 °C with [¹¹C]biotin in PBS (0.56 nmol of biotin, NBA), vehicle (PBS solution, no-[¹¹C]biotin-added) and 0.1 mM [¹¹C]biotin in PBS (biotin added). The streptavidin magnetic particles and supernatant were separated, and the streptavidin magnetic particles washed three times with PBS solution. The radioactivity content in all the tubes was measured using an automated well counter. Streptavidin binding was calculated as the percentage of the total radioactivity bound to the streptavidin magnetic particles after the washing. Control experiments were performed by replacing the streptavidin magnetic particles with solvent buffer.

[¹¹C]biotin-streptavidin binding assay

Avidin and streptavidin have a strong avidity for biotin. The large association constant of the streptavidin-biotin interaction (10-15 M) has driven the use of radiolabeled biotin to track streptavidin in preclinical and clinical setting. [¹¹C]biotin was assayed for streptavidin binding by mixing the radiolabeled compound with streptavidin magnetic beads for 10 minutes at room temperature. After separating the supernatant and washing the beads, it was found that 95.4 ± 0.6% of [¹¹C]biotin bound specifically to the immobilized streptavidin

(**Figure S3**). Incubation with excess of unlabelled biotin reduced [¹¹C]biotin retention to background level (0.5 ± 0.4%).

Biodistribution and metabolite studies in mice

Biodistribution studies were performed to the group of animals receiving [¹¹C]biotin IV. Tissues including brain, cerebellum, heart, lungs, stomach, liver, spleen, small intestine, kidneys, thigh bone and eyes were excised. Blood was also collected. All samples were weighed, and radioactivity content measured using an automated well counter with a standard dilution of [¹¹C]biotin. Counts were decay-corrected and the % of injected dose/gram of tissue (%ID/g) calculated (**Figure S9**).

The urine was analysed with a Thin Layer Chromatography (TLC) plate and a mobile phase of butanol/acetic acid/water (4:1:1 v/v/v). The plate was dried and exposed to phosphor imaging plates for 20 minutes and then scanned in a Typhoon 8600 phosphorimager (GE Healthcare). This analytical method has been reported by McCormick *et al.* which is able to separate biotin (R_f=0.82), bisnorbiotin (R_f=0.72) and biotin sulfoxide (R_f=0.62) in the urine.¹

Uptake and Excretion Clearances of [¹¹C]biotin

Hepatic, renal, BAT, brain uptake clearances (CL_{uptake,liver}, CL_{uptake,kidney}, CL_{uptake,BAT}, CL_{uptake,brain}) of [¹¹C]biotin were measured from 0.3 to 4 min after tracer injection using the previously described integration plot method²⁻⁶ and the following equation:

$$\frac{C_{tissue,t}}{C_{blood,t}} = CL_{uptake} \frac{AUC_{blood,t}}{C_{blood,t}} + c$$

where C_{tissue,t} is the amount of radioactivity per gram tissue in liver, kidney, BAT, brain at time t, and C_{blood,t} is the radioactivity concentration in the left ventricle of the heart at time t. AUC_{blood,t} represents the area under the concentration-time curve in the left ventricle of the heart from time 0 to time t.

Statistical analysis for Figure S9 and Table S3

Biodistribution data and organ to blood data were analysed in SPSS (IBM SPSS Statistics, Version 24.0). using a linear mixed model to explore main and interaction effects of group and organ. Post hoc pairwise tests corrected for multiple comparisons were performed to explore differences between groups in the different organs following significant group and organ interaction effects (p<0.05).

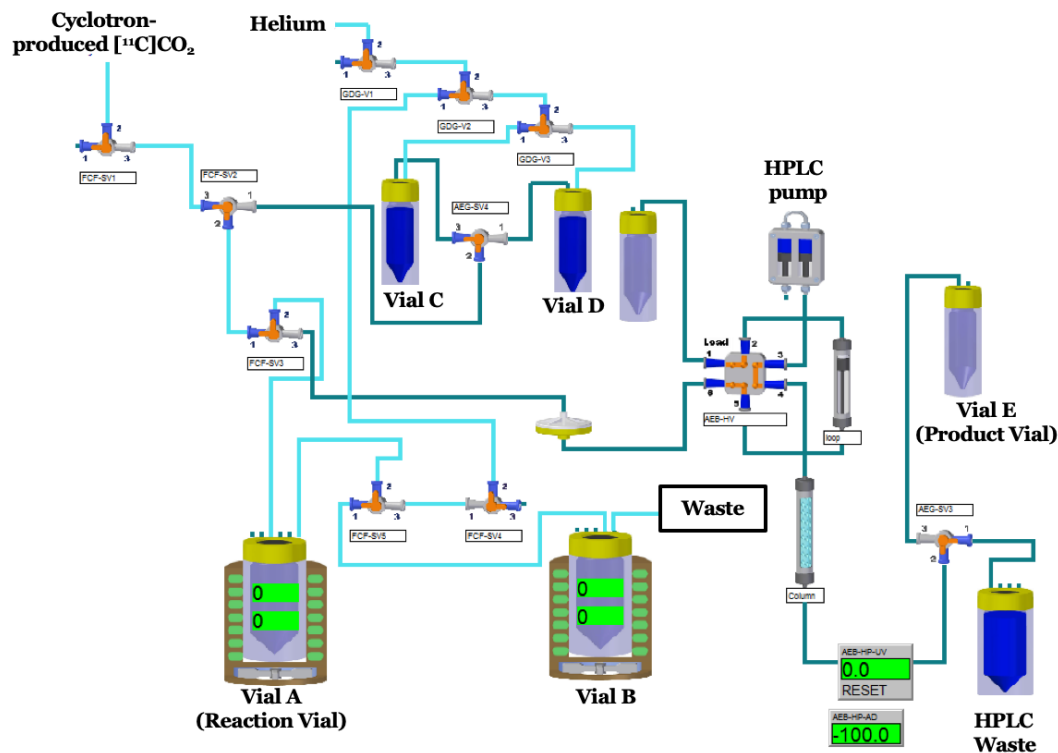


Figure S1: Schematic diagram of the automated synthesis of $[^{11}\text{C}]$ biotin.

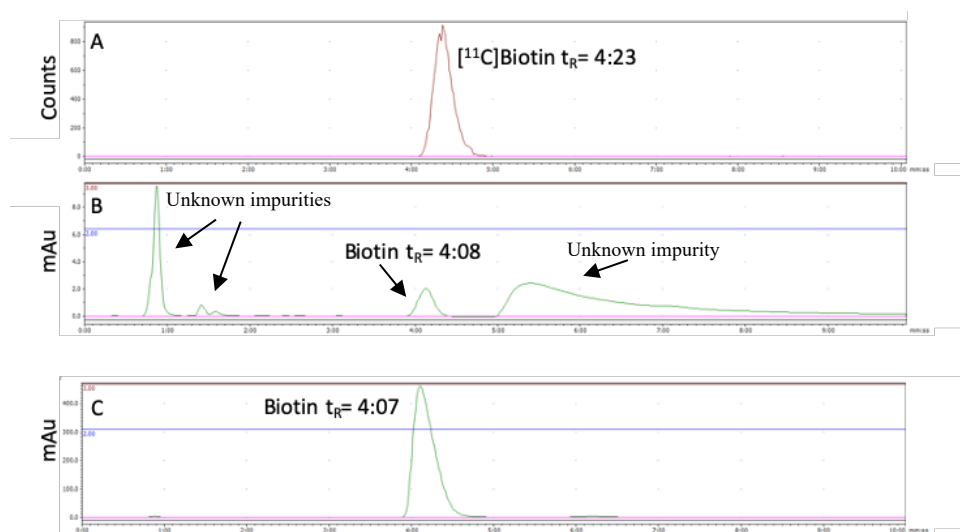


Figure S2 Radio-HPLC radiochromatogram of formulated $[^{11}\text{C}]$ biotin on analytical HPLC.

A Radio-HPLC radiochromatogram $[^{11}\text{C}]$ biotin (retention time (t_R) = 4 minutes and 23 seconds) B) UV-chromatogram of formulated $[^{11}\text{C}]$ biotin (t_R = 4 minutes and 08 seconds) - UV detector ($\lambda = 210$ nm). The difference between UV peaks and radioactivity peaks is 15 seconds and is in the range of delay of this instrument (~ 15 seconds). C) UV chromatogram of biotin (t_R = 4 minutes and 08 seconds).

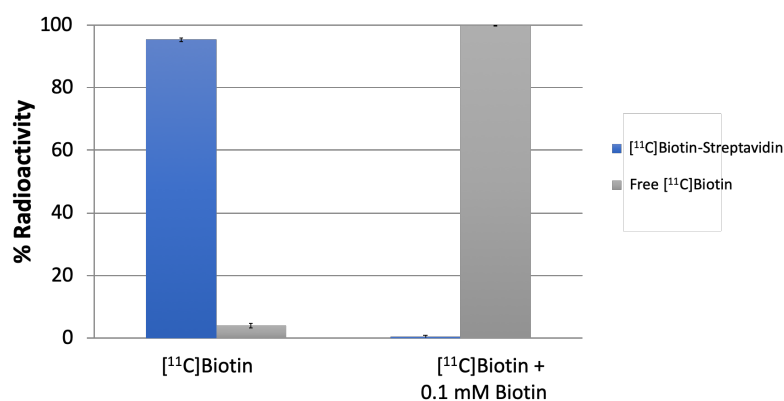


Figure S3: Streptavidin–microspheres uptake of [¹¹C]biotin.

[¹¹C]Biotin was incubated with superparamagnetic particles covalently coupled to streptavidin in the presence of vehicle or biotin (0.1 mM). Blue bars indicated the % of [¹¹C]biotin bound to the streptavidin magnetic beads. Grey bars indicated the % of [¹¹C]biotin found in solution.

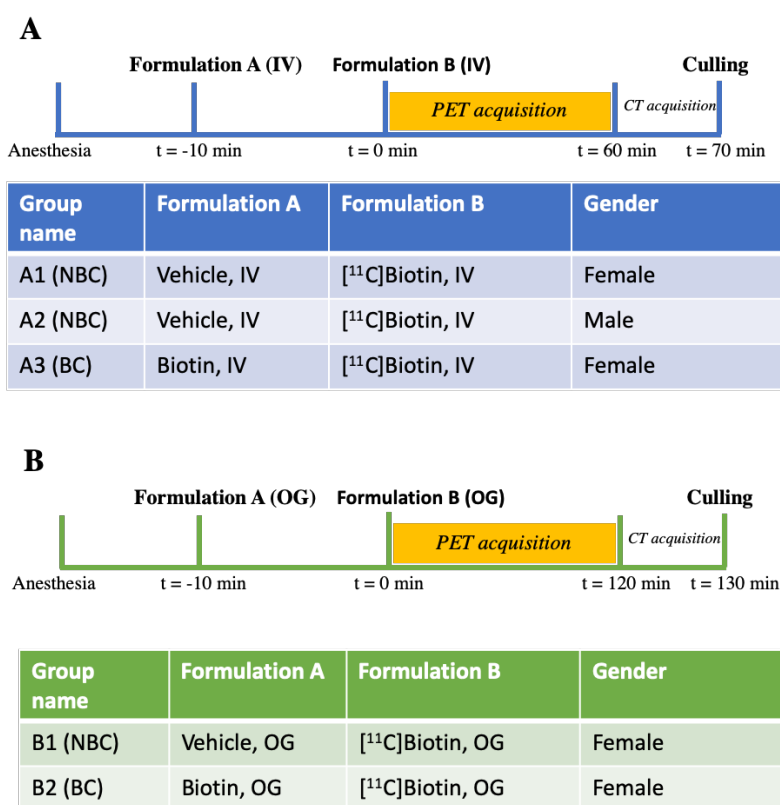


Figure S4. Schematic illustration of the PET/CT image acquisition of intravenous (IV) and orogastric gavage (OG) administration of formulation A and [¹¹C]biotin.

Formulation A: 2.5% ethanol in PBS (groups A1, A2 and B1) or biotin (5 mg/Kg) dissolved in 2.5% ethanol in PBS (groups A3 and B2).

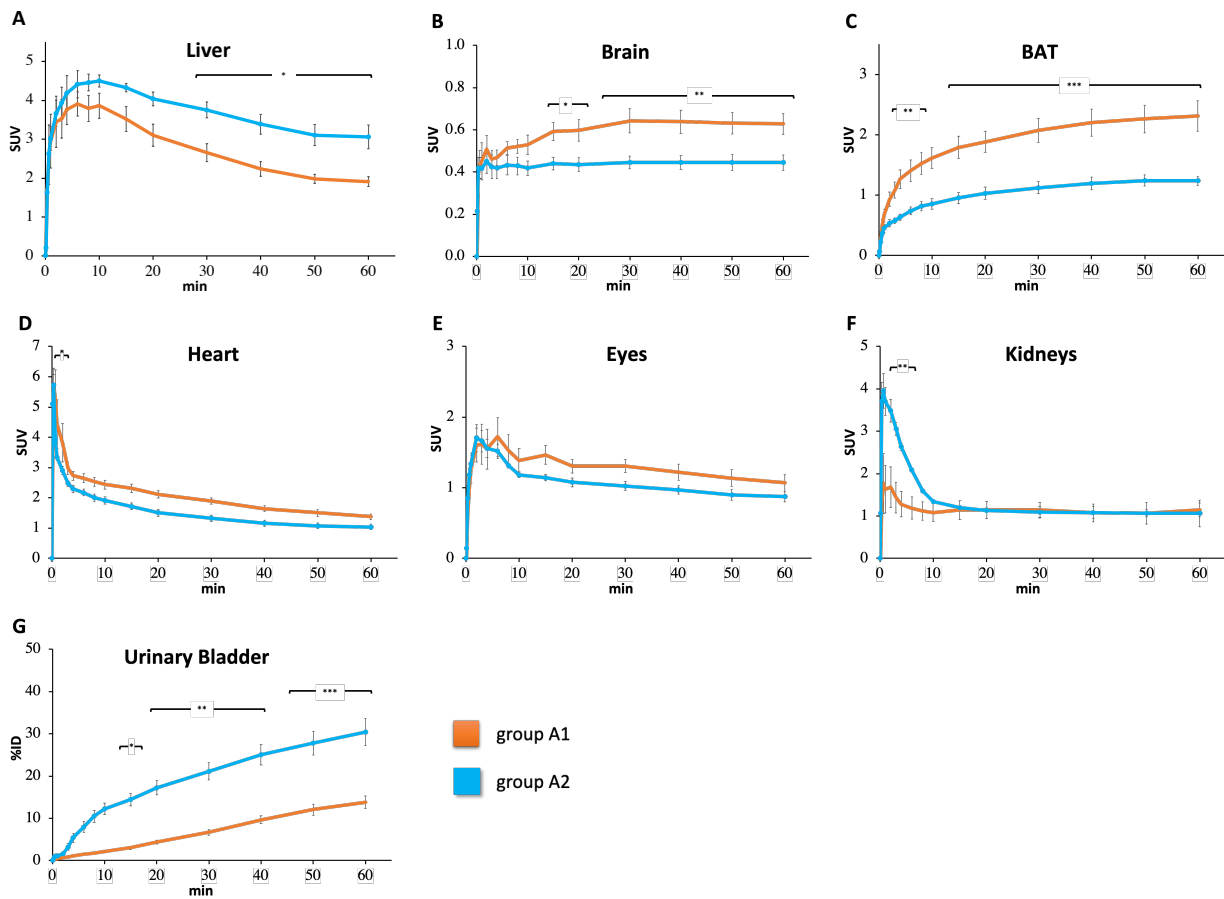


Figure S5: Time Activity curves of male and female mice receiving [¹¹C]biotin IV.

Time-SUV profile (0-60 minutes) of liver (A), brain (B), BAT (C), heart (D), eyes (E), kidneys (F) in female (orange line, group A1) and male (blue line, group A2) NBC mice. The radioactivity of urinary bladder (G) is expressed as % of ID. Data are the mean ± SEM. Note that the y-scale (SUV) varies between the different tissues.

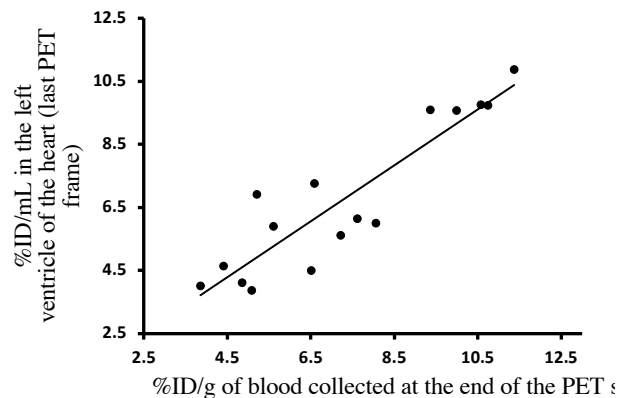


Figure S6 Correlation of blood radioactivity concentration from in vivo PET images versus ex vivo biodistribution.

Correlation of radioactivity concentration (%ID/g) in the left ventricle of the heart measured in the last PET time frame (50-60 min) with radioactivity concentration ((%ID/g) in venous blood collected at the end of the PET scan measured in a gamma counter. Solid line represents linear regression fit ($r = \text{Pearson correlation coefficient} = 0.91$, $P \text{ value} < 0.0001$).

$$\frac{AUC_{tissue,t}}{C_{tissue,t}} = V_T \frac{AUC_{blood,t}}{C_{tissue,t}} + q$$

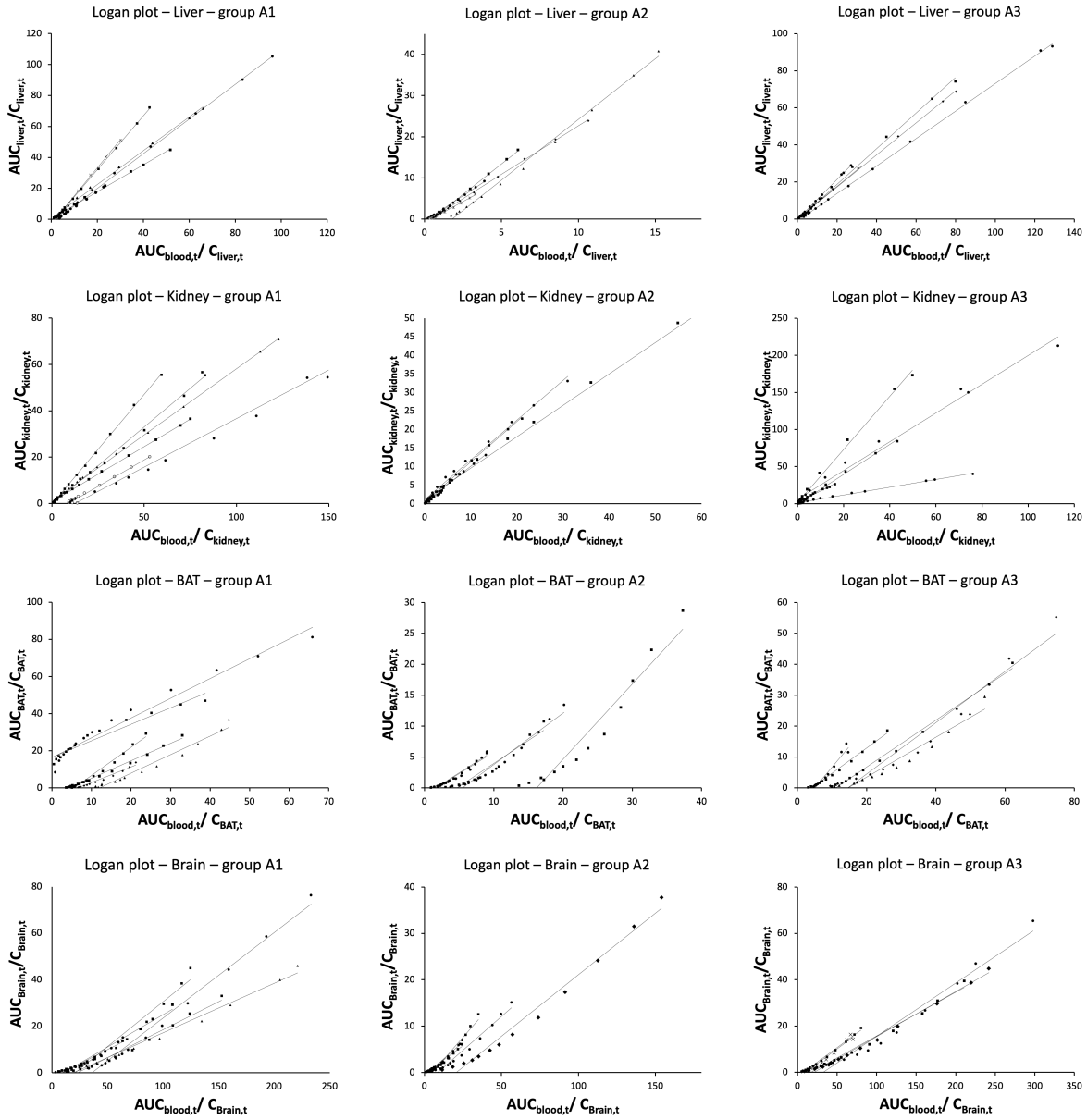


Figure S7 Logan equation and Logan plots of kidney, liver, BAT and brain of groups A1-A3.

$$\frac{C_{tissue,t}}{C_{blood,t}} = K_i \frac{AUC_{blood,t}}{C_{blood,t}} + c$$

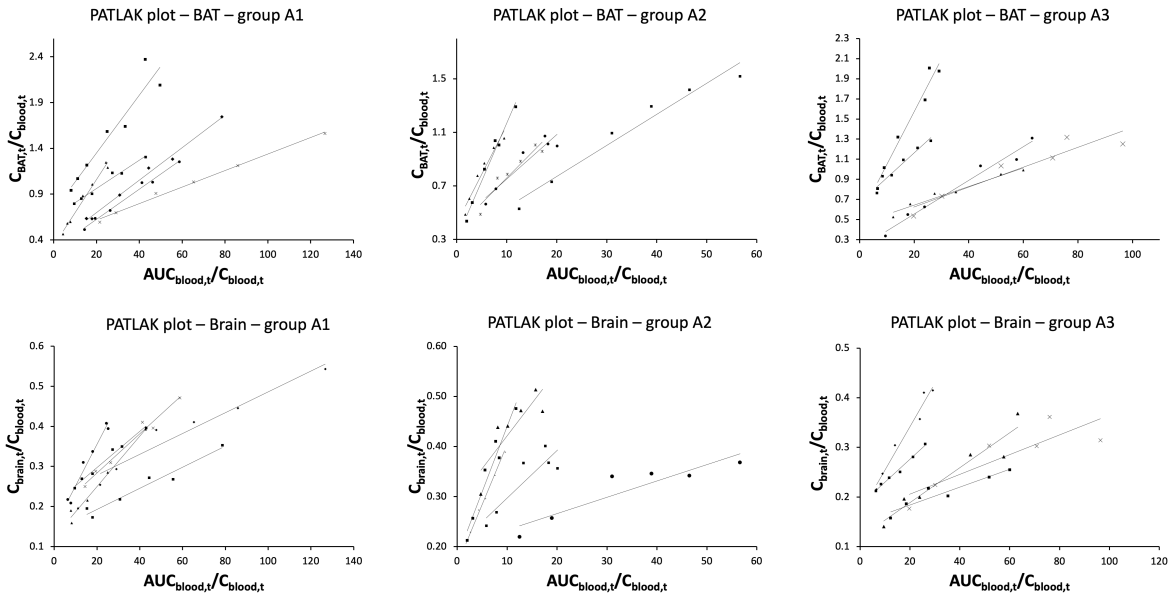


Figure S8 Patlak equation and Patlak plots of BAT and brain of groups A1-A3.

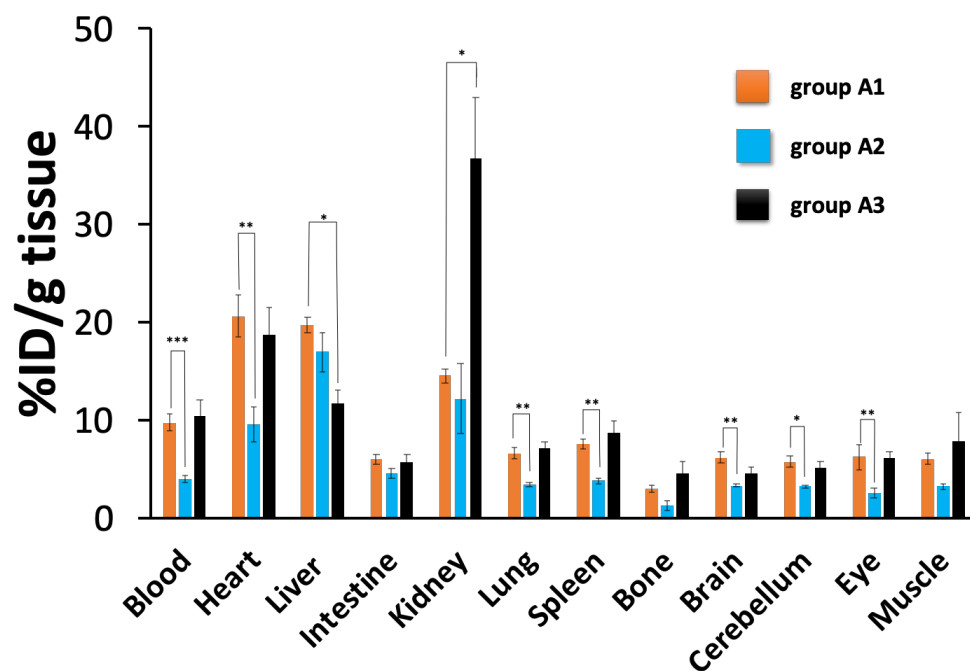


Figure S9: Biodistribution of radio activity after injection of [¹¹C]biotin in mice.

Biodistribution results at 70 minutes (normalized to a 20 g mouse) post-injection of [¹¹C]biotin in female NBC mice (orange, group A1, n=6), male NBC mice (blue, group A2, n=5) and female BC mice (black, group A3, n=5). Data are expressed as %ID/g, mean ± SEM. Data of groups A2 and A3 compared to control group A1 were indicated with (*) for p < 0.05, (**) for p < 0.01, and (***) for p < 0.001.

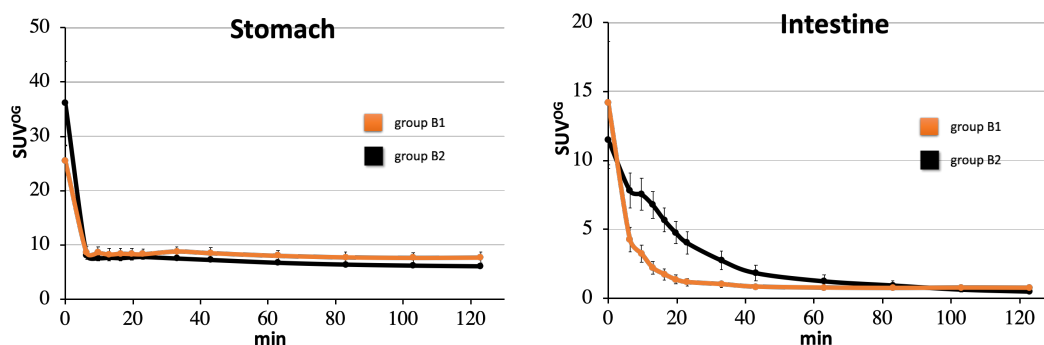


Figure S10: Time Activity curves of female mice receiving [¹¹C]biotin OG.

Time-SUV profile (0-60 minutes) of stomach (A) and intestine (B) in NBA female (orange line, group B1) and BC male (black line, group B2) mice. Data are the mean ± SEM.

Table S1: Details of [¹¹C]biotin synthesis.

Cyclotron-delivered [¹¹C]CO₂ radioactivity	5.9 ± 0.3 GBq
n	26
A_m at EOD	7 ± 1 GBq/μmol
Activity yield – non decay corrected	6 ± 1%
Isolated RCY	19 ± 2%
Radiochemical purity (RCP)	>99%
Radioactivity in 200 μL at EOS	18 ± 2 MBq
Production time from EOD	32 ± 1 minutes

Table S2: Details of [¹¹C]biotin formulation administered to animal groups.

Group	A1	A2	A3	B1	B2
Administration of [¹¹C]biotin	IV	IV	IV	OG	OG
Administration of vehicle or biotin	IV (vehicle)	IV (vehicle)	IV (biotin)*	OG (vehicle)	OG (biotin)*
Gender	Female	Male	Female	Female	Female
Number of animals	6	5	5	5	5
Weight (g)	17 ± 1	24 ± 1	17 ± 1	20 ± 1	20 ± 1
A_m at EOD	5.8 ± 1.1	7.5 ± 0.6	7.1 ± 2.0	7.7 ± 1.4	6.9 ± 2.0
A_m at start of PET imaging study	0.5 ± 0.1	0.7 ± 0.2	0.7 ± 0.3	0.8 ± 0.2	0.8 ± 0.2
Time from EOD to start of PET Imaging study	68 ± 5	69 ± 7	71 ± 5	68 ± 7	61 ± 2
μg of biotin in the [¹¹C]biotin formulation	1.6 ± 0.4	1.6 ± 0.2	1.7 ± 0.6	1.8 ± 0.3	1.7 ± 0.5
μg/kg of biotin administered	98 ± 28	67 ± 9	97 ± 35	94 ± 16	83 ± 21
Activity administered (MBq)	3.3 ± 0.5	6.5 ± 1.6	3.0 ± 0.8	8.3 ± 2.2	5.1 ± 1.1

*Groups A3 and B2 received 5 mg/kg of biotin 10 minutes before the administration of [¹¹C]biotin.

Table S3: Tissue/Blood Ratio for groups A1-A3.

	Group A1	Group A2	Group A3
Heart	2.1 ± 0.7	2.4 ± 1.1	1.8 ± 0.9
Liver	2.0 ± 0.5	4.2 ± 1.7***	1.1 ± 0.6*
Intestine	0.6 ± 0.2	1.1 ± 0.3***	0.6 ± 0.3
Kidney	1.5 ± 0.4	3.0 ± 2.8	3.6 ± 2.3
Lung	0.7 ± 0.2	0.8 ± 0.2	0.7 ± 0.3
Spleen	0.8 ± 0.2	0.9 ± 0.2	0.8 ± 0.4
Bone	0.3 ± 0.1	0.3 ± 0.3	0.4 ± 0.3
Brain	0.6 ± 0.2	0.8 ± 0.2	0.4 ± 0.2
Cerebellum	0.6 ± 0.2	0.8 ± 0.2**	0.5 ± 0.2
Eye	0.6 ± 0.4	0.7 ± 0.4	0.6 ± 0.3
Muscle	0.6 ± 0.2	0.8 ± 0.2	0.8 ± 0.7

Data of groups A2 and A3 compared to control group A1 were indicated with (*) for $p < 0.05$, (**) for $p < 0.01$, and (***) for $p < 0.001$.

References

- (1) Lee, H. M.; Wright, L. D.; McCormick, D. B. Metabolism of carbonyl-labeled ^{14}C -biotin in the rat. *J Nutr* **1972**, *102*, 1453-1463.
- (2) Traxl, A.; Wanek, T.; Mairinger, S.; Stanek, J.; Filip, T.; Sauberer, M.; Muller, M.; Kuntner, C.; Langer, O. Breast cancer resistance protein and p-glycoprotein influence in vivo disposition of ^{11}C -erlotinib. *J. Nucl. Med.* **2015**, *56*, 1930-1936.
- (3) Takashima, T.; Wu, C.; Takashima-Hirano, M.; Katayama, Y.; Wada, Y.; Suzuki, M.; Kusuhara, H.; Sugiyama, Y.; Watanabe, Y. Evaluation of breast cancer resistance protein function in hepatobiliary and renal excretion using PET with ^{11}C -SC-62807. *J. Nucl. Med.* **2013**, *54*, 267-276.
- (4) Takashima, T.; Nagata, H.; Nakae, T.; Cui, Y.; Wada, Y.; Kitamura, S.; Doi, H.; Suzuki, M.; Maeda, K.; Kusuhara, H.; Sugiyama, Y.; Watanabe, Y. Positron emission tomography studies using (15R)-16-m- ^{11}C tolyl-17,18,19,20-tetranorisocarbacyclin methyl ester for the evaluation of hepatobiliary transport. *J. Pharmacol. Exp. Ther.* **2010**, *335*, 314-323.
- (5) Shingaki, T.; Hume, W. E.; Takashima, T.; Katayama, Y.; Okauchi, T.; Hayashinaka, E.; Wada, Y.; Cui, Y.; Kusuhara, H.; Sugiyama, Y.; Watanabe, Y. Quantitative evaluation of mMatel1 function based on minimally invasive measurement of tissue concentration using PET with ^{11}C metformin in mouse. *Pharm. Res.* **2015**, *32*, 2538-2547.
- (6) Takano, A.; Kusuhara, H.; Suhara, T.; Ieiri, I.; Morimoto, T.; Lee, Y. J.; Maeda, J.; Ikoma, Y.; Ito, H.; Suzuki, K.; Sugiyama, Y. Evaluation of in vivo p-glycoprotein function at the blood-brain barrier among MDR1 gene polymorphisms by using ^{11}C -verapamil. *J. Nucl. Med.* **2006**, *47*, 1427-1433.